

**Novel application of chain transfer agents for generation of high value polymers  
during mechanical recycling.**

*By*

Gwen Wilusz

John Estock, Megan Hill

A thesis submitted in partial fulfilment of the requirements for graduation with distinction

University Honors Program

Department of Chemistry

College of Natural Sciences

Colorado State University

Fall 2024

Advisor: Megan R. Hill, Ph.D.

Committee Member: Claudia Boot, Ph.D.

*December 13, 2024*

## **Abstract**

Plastic consumption has increased drastically in the modern era, inevitably leading to an increase in plastic waste. While recycling was historically proposed to counteract this influx, the combination of the heating and shearing forces innate to this process leads to the formation of highly reactive, short-lived radical species that can induce chain degradation of polymers. This decreases the overall molecular weight of the material, inevitably resulting in lower-value products. This work demonstrates improvements that will increase the mechanical recyclability of polymer waste by introducing accessible functionality to degraded polymers through mechanoradical capture. Trithiocarbonate (TTC) chain transfer agents (CTAs), typically used in reversible addition fragmentation chain transfer (RAFT) polymerizations, have the unique ability to stabilize and capture radicals. Thus, introducing these small molecules during the mechanical recycling process captures the mechanoradicals formed, effectively functionalizing the waste polymers. These functionalized polymers are then employed as macroinitiators for controlled polymerization. In addition, TTC functionalities are used as labile groups that allow for depolymerization to monomer at more accessible temperatures. This novel method generates both higher molecular weight materials akin to virgin polymers and produces monomers that can be repolymerized, offering a promising path toward a circular plastic economy.

## Introduction

Polymeric materials have become indispensable in modern life and are integral in everyday products from clothing to tires. Largely due to this versatility, plastic waste has increased almost 300% in the United States over the past 40 years.<sup>1</sup> However, there is a lack of sustainable end-of-life options to counteract this influx, as only 9% of the plastic ever made has been recycled.<sup>2</sup> While the inherent stability of polymeric materials is a desirable property for performance, it hinders the ease of degradation. Hence, landfills become saturated, and waste accumulates. Additionally, because of the poor recycling rate of polymeric materials,<sup>2</sup> new polymers need to be synthesized, increasing our dependence on the fossil fuels from which most monomers are derived.

While recycling was historically proposed to minimize plastic waste build up, difficulty in plastic sorting, contamination from additives, and chain scission from heating and shearing forces ultimately leads to the downcycling of materials that survive the recycling process.<sup>3</sup> One of the many problems with mechanical recycling is chain degradation resulting from the formation of highly reactive, short-lived radical species that form under mechanical force. These mechanoradicals can lead to chain scission, chain branching, and crosslinking – both decreasing overall molecular weight and increasing polydispersity.<sup>4,5</sup> Because materials properties are dependent on molecular weight, such scission events inevitably result in downcycling to lower value products.

It is well established in the field of polymer science that the fracture of polymer chains results in radical formation.<sup>6-11</sup> There is continuous fracture of polymer chains, and the resultant radical species terminate through various pathways. While termination leads to shorter chains, a variety of chemistries have been used to capture the active radical species before termination. For example, ball milling has been used to fluorescently label polymers through the capture of radicals formed during chain scission.<sup>12</sup> Additionally, low ceiling temperature polymers have been functionalized with phthalimide moieties through mechanoradical capture during ultrasonication (Figure 1).<sup>13</sup> This phthalimide functionality has recently been found to lower ceiling temperatures for depolymerization.<sup>13,14</sup> Mechanoradical species have also been shown to catalyze reactions. Polyethylene

mechanoradicals produced under ball milling have been used to catalyze the dehalogenation of various small molecules.<sup>15</sup> Alternatively to radical termination and capture pathways, Choi and coworkers have recently shown radical depropagation of polymethacrylates through ball milling.<sup>16</sup> This method achieved up to 40% depolymerization to monomer in the presence of minimal solvent, as well as molecular weights <1 kDa.<sup>16</sup>

### Previous Work

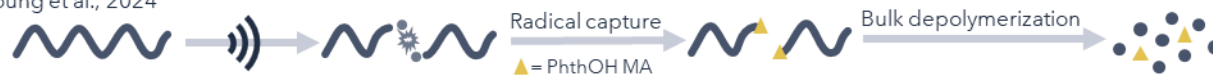
Bartsch and Schmidt-Naake, 2006



Stache et al., 2020



Young et al., 2024



### This Work

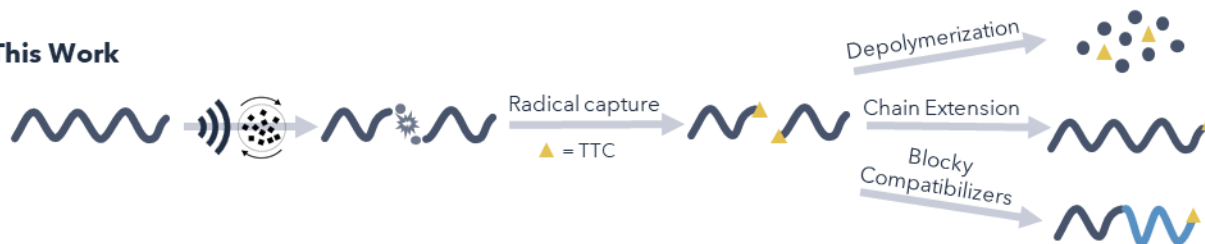


Figure 1. Previous work using polymer radical capture for chain extension or bulk depolymerization of commodity polymers. This work, using ultrasonication and ball milling for mechanoradical capture using TTCs for applications in chain extension and bulk depolymerization.

We wondered if we could similarly capture these radicals being formed under mechanical force with small molecule chain transfer agents (CTAs) to enable better reuse and recycling of polymers. We were inspired by the work by Stache and Fors<sup>17</sup> using bis(thiocarbonyl) disulfide compounds, typically precursors to traditional reversible addition fragmentation chain transfer (RAFT) agents, to capture radicals formed on small molecules and polymers formed from hydrogen atom transfer (HAT) reactions. Specifically, by functionalizing polymers with trithiocarbonates (TTCs) using radical capture, this work was able to then chain extend and create grafted polymers (Figure 1).<sup>17</sup> In addition, TTCs have been shown to decrease the ceiling temperature for depolymerization.<sup>14,18</sup> We hypothesized that bis(thiocarbonyl) disulfides could similarly capture radicals formed under

mechanical force and enable chain-extension or decreased ceiling temperatures from “waste” plastics.

Previous work using ultrasonication has captured mechanoradicals using either nitroxide species or copper halides to cap polymer chains.<sup>19,20</sup> Using either functionality, both works were able to chain extend the resulting macroinitiators to form block copolymers (Figure 1).<sup>19,20</sup> We wondered if we could extend this concept to TTCs using RAFT polymerization. There are many benefits to RAFT polymerization including a large monomer scope, moderate temperatures, high end group fidelity, as well as a living chain end.<sup>21</sup> TTCs allow for an equilibrium between active and deactivated chains, resulting in a living, controlled polymerization. Due to their role of radical stability in RAFT polymerizations, we hypothesized that TTC CTAs could capture radicals formed under mechanical force.

While ultrasonication results in narrow dispersities of the resultant degraded polymers, this technique has many limitations. Ultrasonication relies on the formation and subsequent collapse of cavitation bubbles in solution to cause homolytic cleavage of polymer chains. Thus, this technique is severely limited by concentration due to the inherent viscosity of polymers. Ultrasonication must be performed in exceedingly dilute solution. By utilizing ball milling, polymers can be degraded without the use of solvent and in the bulk.

Herein, we describe the mechanical degradation, radical capture, and repolymerization of poly(methyl methacrylate) (PMMA) and polystyrene (PS) using ultrasonication and ball milling.

## Results and Discussion

We first studied the degradation of PMMA and PS under ultrasonication and ball milling conditions. Ultrasonication results in fracture due to the collapse of cavitation bubbles in solution pulling the polymer chain ends. This consistently leads to breakage in the middle of a chain, resulting in narrow dispersities. For example, when starting with 280 kDa PS with a PDI of 1.9, ultrasonication consistently resulted in molecular weights near 80 kDa and PDIs of 1.1 (Figure 2a). In addition, a plateau of degradation is consistently observed where the ultrasonicated polymers reach a limiting molecular weight around 70 kDa even after increasing the reaction time by several hours. Consistent with literature reports, we found that ultrasonication requires dilute conditions ( $5 \text{ mg mL}^{-1}$ ).

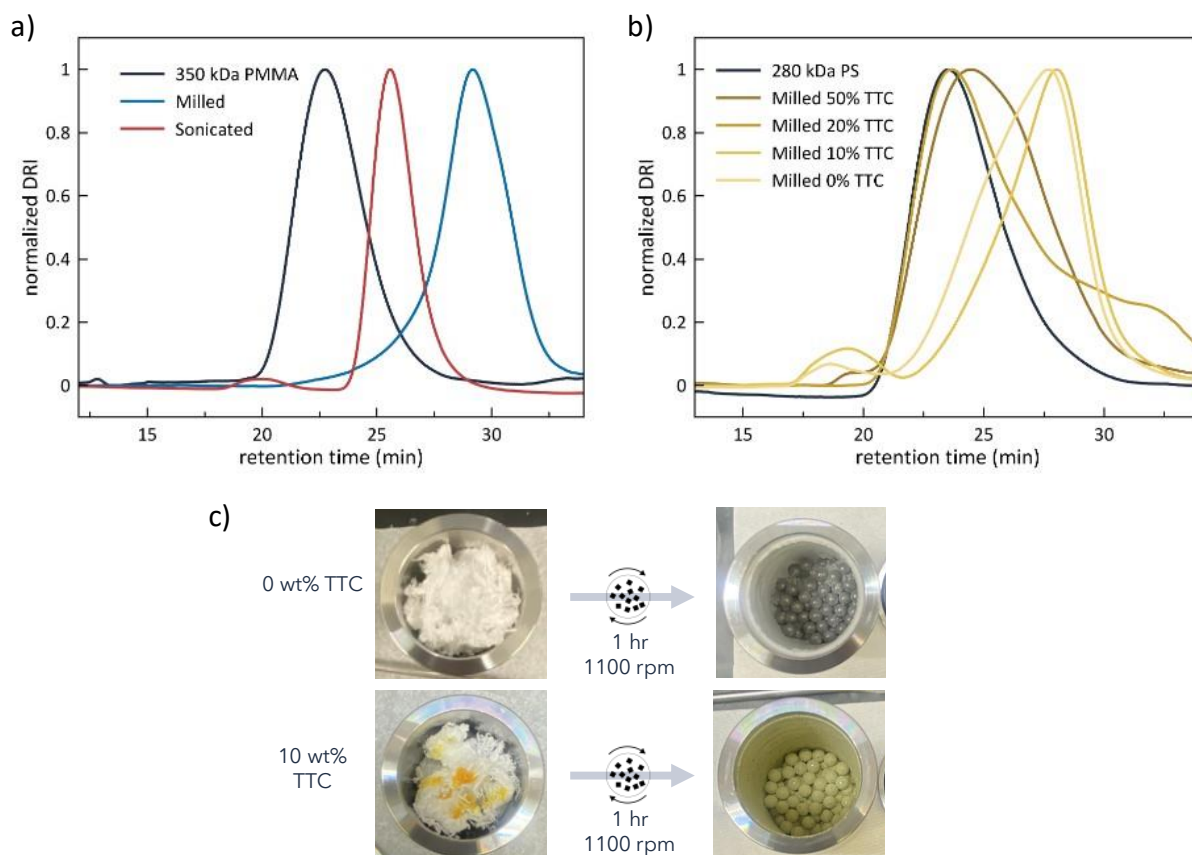


Figure 2. (a) SEC chromatograms showing the differential refractive index (DRI) of 350 kDa PMMA after ball milling and ultrasonication. (b) DRI traces exhibiting the differences in chain degradation of PS after ball milling with various wt% of TTC. (c) PS before and after ball milling at standard conditions.

In contrast to ultrasonication, ball milling uses the centrifugal force of balls in a jar to physically grind down polymers. Thus, ball milling has more chain scission events depending on where the polymer chain is impacted. This leads to a more disperse distribution of

polymers, but also allowed us to reach molecular weights as low as 30 kDa, with literature reported molecular weights as 1 kDa (Figure 2a).<sup>16</sup> Despite the difference in mechanism for inducing chain scission, ball milling also had reproducible results. For example, when milling 350 kDa PMMA with a PDI of 1.7, ball milling consistently produced molecular weights near 9 kDa with PDIs of 1.5 when all parameters were held constant. In addition, milling constantly mixes the reaction – decreasing barriers to reaction from diffusion.<sup>22</sup>

With the addition of TTCs, polymer degradation was significantly suppressed under ball milling conditions. As seen in Figure 2b, when above 10 wt% of TTC was added to the reaction vessel, degradation was inhibited almost completely, with  $M_w$  remaining above 200 kDa (Figure 2b, S8, Table S4). We hypothesized that this was due to the liquid texture of bis(butyl trithiocarbonate), as it has previously been shown that liquid-assisted grinding (LAG) of polymethacrylates can inhibit degradation.<sup>16</sup> As the concentration of TTC was decreased from 50 wt% to 10 wt%, molecular weights approached 70 kDa and a percent TTC incorporation of around 0.4 wt% were achieved (Figure 2b,2c, Table S4). To test this hypothesis, we also milled the PMMA with varying amounts of t-butanol. We classified these conditions on the  $\eta$ -scale which describes the ratio of volume of solvent to mass of solute. An  $\eta$ -value of 0-1 constitutes LAG, while an  $\eta$ -value of 1-10 constitutes slurry-assisted grinding.<sup>23</sup> We found that both  $\eta = 0.1$  and  $\eta = 3.33$  ( $\mu\text{L mg}^{-1}$ ) conditions prevented degradation of the polymer.<sup>23</sup> Thus, both liquid and slurry conditions resulted in a decrease in chain scission events, and limited polymer functionalization with TTC.

We also hypothesized that the addition of monomer could increase the lifetime of radicals formed (through propagation of the radical), thereby increasing the potential for CTAs to add to the fragmented chain. In addition, this could aid in limiting the formation of primary radicals that, when captured by TTC, would not be able to chain extend. Using optimized volumes of monomer ( $\eta = 0.076$ ), degradation was comparable to neat conditions without significant LAG effects. While TTC incorporation was on average 0.4 wt% without any monomer present during ball milling, it decreased to 0.26 wt% with the addition of monomer. While overall TTC incorporation decreased, further experiments need to be performed to determine if the effect on proportion of active TTC chain ends.

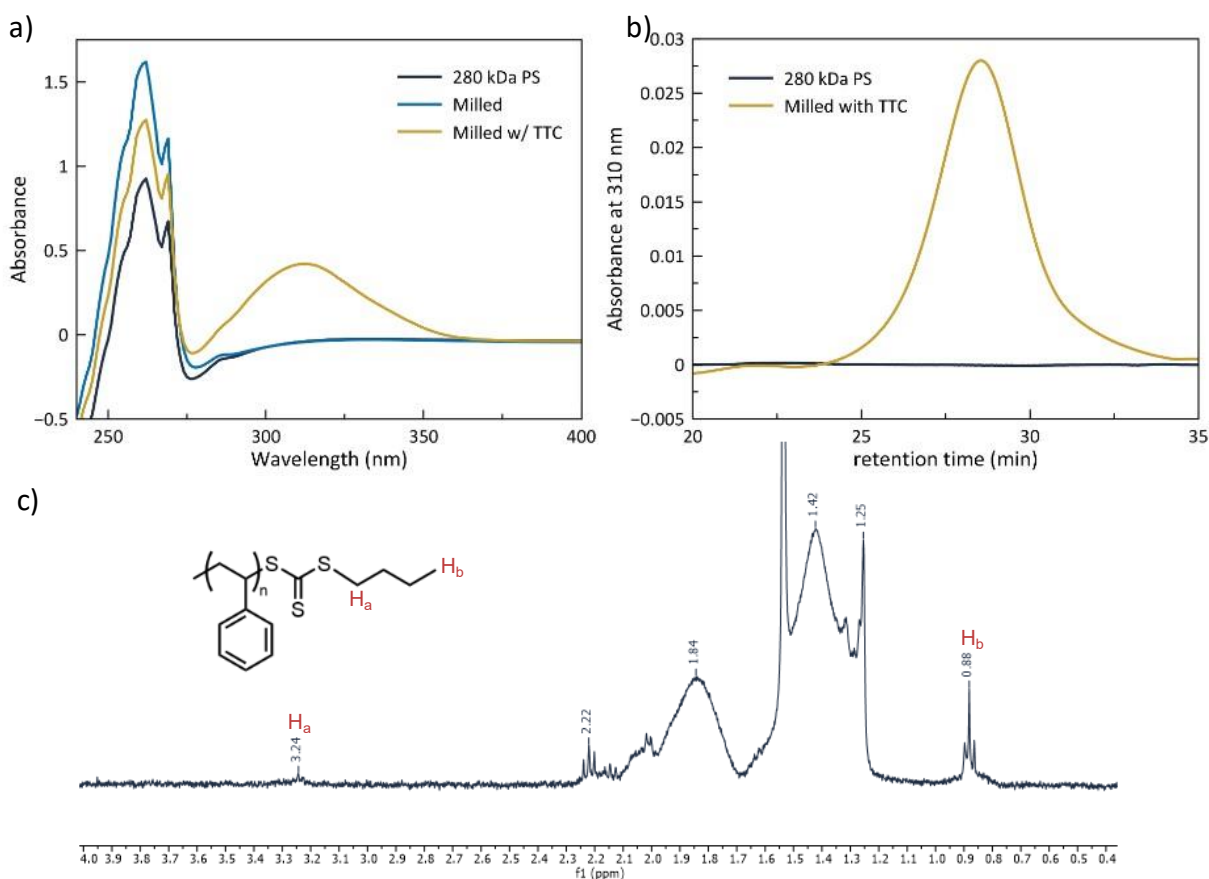


Figure 3. (a) Absorbance profiles of 280 kDa PS before milling, after milling, and after milling with TTC. (b) UV absorbance at 310 nm measured with SEC of 280 kDa PS before milling, and after milling with TTC. (c)  $^1H$ -NMR spectrum of PS after milling with TTC.

Functionalization of the degraded polymers was confirmed using UV/Visible spectroscopy, thermal gravimetric analysis (TGA) coupled with mass spectrometry (MS), and proton nuclear magnetic resonance (NMR) spectroscopy (Figure 3). TTCs uniquely absorb strongly at 310 nm, while both PMMA and PS do not (Figure 3a). Thus, we were able to take

advantage of the unique spectroscopic characteristics of TTC to both qualitatively and quantitatively determine functionalization. UV/Vis spectroscopy coupled with size exclusion chromatography (SEC-UV) showed an increase of UV signal at 310 nm at low molecular weights, confirming the presence of TTC functionality on the chain end (Figure 3b). We were able to quantify the functionality by making a calibration curve from synthesized low molecular weight polymers with a known concentration of TTC chain ends and plotting their absorption at 310 nm at various concentrations (Figure S15). SEC-UV allowed for further confirmation that any absorbance quantified was due to the polymer itself rather than residual bis(TTC) small molecules in solution. In addition to UV/Vis spectroscopy, protons associated with the TTC were visible by NMR (Figure S7). However, due to low resolution, the degree of functionalization could not be reliably estimated by their relative integration compared to the polymer chain (Figure 3c). Lastly, CS<sub>2</sub>, a fragment of the TTC chain end, was consistently observed by TGA-MS and could be further quantified by integrating its relative abundance.

After the successful demonstration of mechanoradical capture during ball milling and ultrasonication of PS and PMMA by TTCs, RAFT polymerizations were then performed to chain extend the degraded polymers. Various control experiments were performed on both model polymers with known TTC end groups and degraded polymers that were unfunctionalized to demonstrate that chain extension could occur but only in the presence of a TTC end group (Figure S13, S14). Blue light polymerizations were used to mitigate the need for an exogenous initiator. Excitingly, the degraded macroinitiators were successfully chain-extended to target their original molecular weights before mechanical degradation as demonstrated in Figure 4a (Table S8). To test the chain-extended macroinitiator properties, we scaled up the ball milling reactions. While this resulted in a smaller reduction in

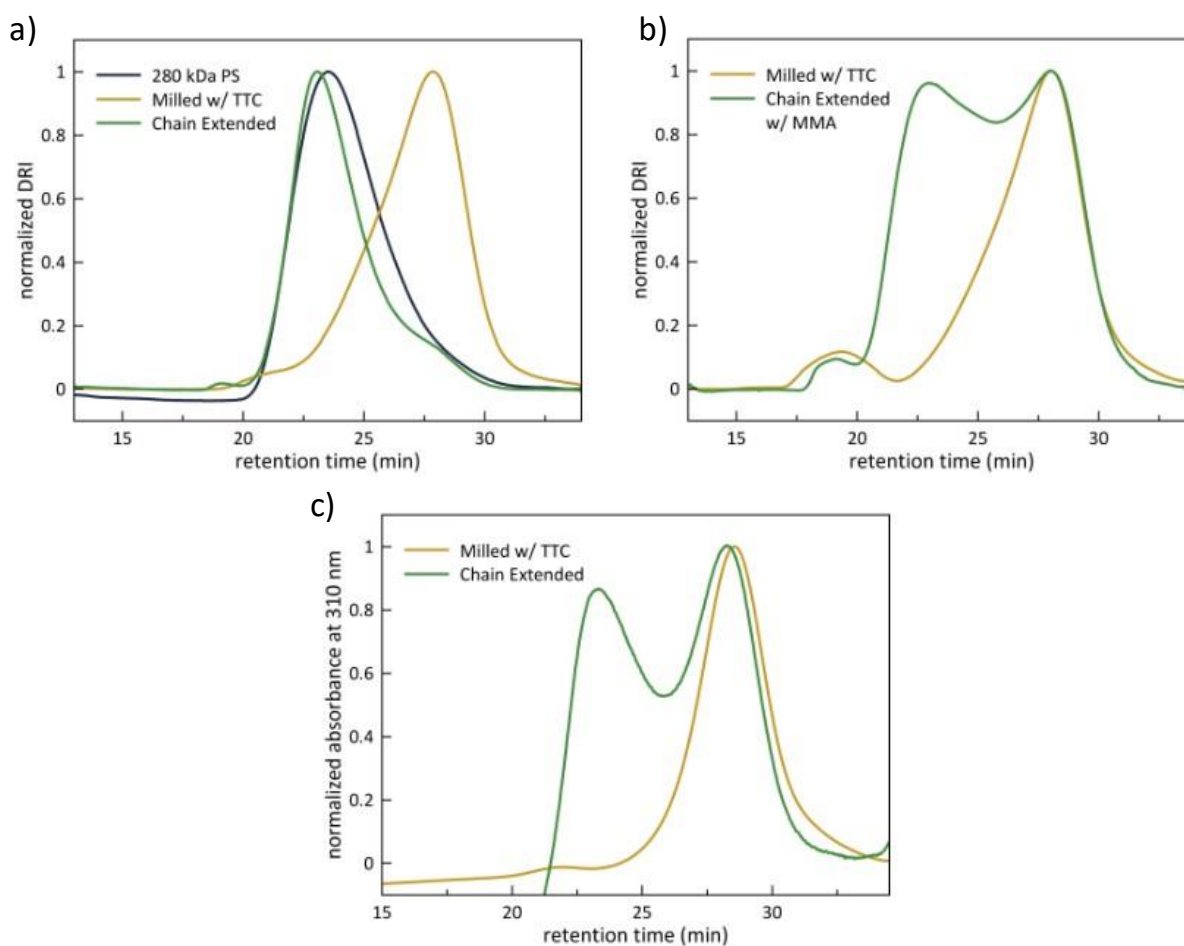


Figure 4. (a) SEC of macroinitiator PS chain extended by RAFT polymerization to its original molecular weight. (b) SEC of macroinitiator PS copolymerized with MMA to form a deblock polymer. (c) SEC-UV spectrum showing absorbance at 310 of macroinitiator and chain extended PS.

molecular weight, the polymer still degraded significantly, and similar TTC incorporations were observed.

In addition to homopolymerizations, degraded TTC-functionalized polymers were copolymerized, demonstrating a novel way to synthesize block copolymers. Polystyrene-block-poly(methyl methacrylate) and poly(methyl methacrylate)-block-polystyrene were synthesized using this method (Figure 4b). Chain extension of PS with MMA had low efficiency that could be contributed to the innate electronics of the chosen monomers. However, further investigations are being carried out to explore the performance of poly(methyl methacrylate)-block-polystyrene in compatibilization applications.

Lastly, we have begun to explore if the incorporation of both TTC and unsaturated moieties on PMMA allowed for thermal depolymerization to monomer at lower temperatures. We have had conflicting results with the literature and found that PMMA milled with TCC had a higher  $T_{95}$  than its virgin counterpart (Figure 5). Excitingly preliminary results show that milling with monomer may mitigate the need for TTC radical capture, as PMMA milled with monomer exhibited a significant mass loss around 200°C. Further experiments are being conducted to determine if this method leads to a unique and viable thermal depolymerization pathway.

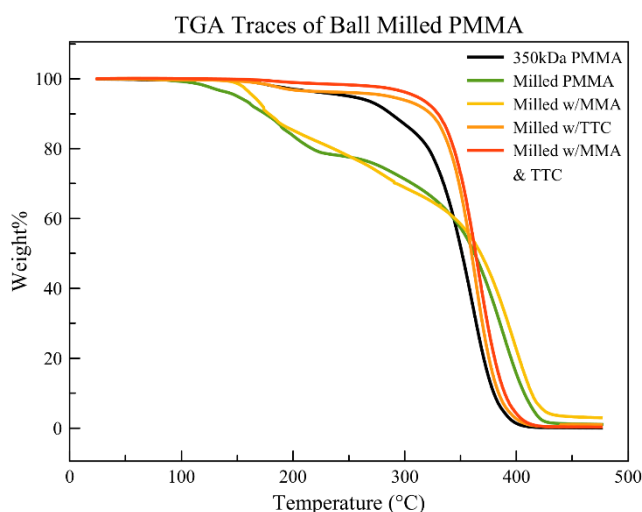


Figure 5. TGA of PMMA milled at different conditions. Those milled with TTC exhibit weight loss much earlier than commercial polymer.

## **Conclusions and Outlook**

We have demonstrated that functionalization through radical capture during mechanical degradation is possible. We achieved ~0.4 wt% functionalization of both PS and PMMA with ball milling in the presence of 10 wt% TTC. This is an efficient and controlled method of introducing functionality to waste polymers. Importantly, we were able to show controlled chain extension by RAFT homopolymerization and copolymerization to achieve targeted molecular weights and restore mechanical properties of the degraded material. We expect that this method can be expanded to other commercial polymers and may serve as a viable route to upcycling plastic waste.

## **Acknowledgements**

I would like to thank my research mentor Dr. Megan Hill for two years of mentoring scientific research and fostering my love for polymer chemistry. I would also like to thank the Hill lab for their support throughout this project, specifically John Estock for performing experiments and furthering the project. Additionally, I would like to thank Dr. Claudia Boot and the employees of the Analytical Resources Core – Materials and Molecular Analysis Division for their continued support throughout my undergraduate career. I have learned invaluable knowledge from you all, and I am so grateful for our friendships.

## References

- (1) *The Real Truth about the US Plastic Recycling Rate*; Beyond Plastics, Bennington College, 2022. [https://static1.squarespace.com/static/5eda91260bbb7e7a4bf528d8/t/62b2238152acae761414d698/1655841666913/The-Real-Truth-about-the-US-Plastic-Recycling-Rate-2021-Facts-and-Figures-\\_5-4-22.pdf](https://static1.squarespace.com/static/5eda91260bbb7e7a4bf528d8/t/62b2238152acae761414d698/1655841666913/The-Real-Truth-about-the-US-Plastic-Recycling-Rate-2021-Facts-and-Figures-_5-4-22.pdf) (accessed 2024-03-14).
- (2) OECD. *Global Plastics Outlook: Economic Drivers, Environmental Impacts and Policy Options*; OECD, 2022. <https://doi.org/10.1787/de747aef-en>.
- (3) Rahimi, A.; García, J. M. Chemical Recycling of Waste Plastics for New Materials Production. *Nat. Rev. Chem.* **2017**, *1* (6), 1–11. <https://doi.org/10.1038/s41570-017-0046>.
- (4) Li, H.; Aguirre-Villegas, H. A.; Allen, R. D.; Bai, X.; Benson, C. H.; Beckham, G. T.; Bradshaw, S. L.; Brown, J. L.; Brown, R. C.; Cecon, V. S.; Curley, J. B.; Curtzwiler, G. W.; Dong, S.; Gaddameedi, S.; García, J. E.; Hermans, I.; Kim, M. S.; Ma, J.; Mark, L. O.; Mavrikakis, M.; Olafasakin, O. O.; Osswald, T. A.; Papanikolaou, K. G.; Radhakrishnan, H.; Sanchez Castillo, M. A.; Sánchez-Rivera, K. L.; Tumu, K. N.; Van Lehn, R. C.; Vorst, K. L.; Wright, M. M.; Wu, J.; Zavala, V. M.; Zhou, P.; Huber, G. W. Expanding Plastics Recycling Technologies: Chemical Aspects, Technology Status and Challenges. *Green Chem.* **2022**, *24* (23), 8899–9002. <https://doi.org/10.1039/D2GC02588D>.
- (5) Schyns, Z. O. G.; Shaver, M. P. Mechanical Recycling of Packaging Plastics: A Review. *Macromol. Rapid Commun.* **2021**, *42* (3), 2000415. <https://doi.org/10.1002/marc.202000415>.
- (6) Kauzmann, W.; Eyring, H. The Viscous Flow of Large Molecules. *J. Am. Chem. Soc.* **1940**, *62* (11), 3113–3125. <https://doi.org/10.1021/ja01868a059>.
- (7) Staudinger, H.; Bondy, H. F. Über Isopren Und Kautschuk, 19. Mitteil.: Über Die Molekülgröße Des Kautschuks Und Der Balata. *Berichte Dtsch. Chem. Ges. B Ser.* **1930**, *63* (3), 734–736. <https://doi.org/10.1002/cber.19300630330>.
- (8) Staudinger, H.; Leupold, E. O. Über Isopren Und Kautschuk, 18. Mitteil.: Viscositäts-Untersuchungen an Balata. *Berichte Dtsch. Chem. Ges. B Ser.* **1930**, *63* (3), 730–733. <https://doi.org/10.1002/cber.19300630329>.
- (9) Staudinger, H.; Heuer, W. Über Hochpolymere Verbindungen, 93. Mitteil.: Über Das Zerreißen Der Faden-Moleküle Des Poly-styrols. *Berichte Dtsch. Chem. Ges. B Ser.* **1934**, *67* (7), 1159–1164. <https://doi.org/10.1002/cber.19340670708>.
- (10) Pike, M.; Watson, W. F. Mastication of Rubber, I. Mechanism of Plasticizing by Cold Mastication. *J. Polym. Sci.* **1952**, *9* (3), 229–251. <https://doi.org/10.1002/pol.1952.120090305>.
- (11) Kuzuya, M.; Kondo, S.; Noguchi, A.; Noda, N. Nature of Mechanoradical Formation and Reactivity with Oxygen in Methacrylic Vinyl Polymers. *J. Polym. Sci. Part B Polym. Phys.* **1992**, *30* (1), 97–103. <https://doi.org/10.1002/polb.1992.090300110>.
- (12) Kubota, K.; Toyoshima, N.; Miura, D.; Jiang, J.; Maeda, S.; Jin, M.; Ito, H. Introduction of a Luminophore into Generic Polymers via Mechanoradical Coupling with a Prefluorescent Reagent. *Angew. Chem. Int. Ed.* **2021**, *60* (29), 16003–16008. <https://doi.org/10.1002/anie.202105381>.
- (13) Young, J. B.; Goodrich, S. L.; Lovely, J. A.; Ross, M. E.; Bowman, J. I.; Hughes, R. W.; Sumerlin, B. S. Mechanochemically Promoted Functionalization of Postconsumer Poly(Methyl Methacrylate) and Poly( $\alpha$ -Methylstyrene) for Bulk Depolymerization. *Angew. Chem. Int. Ed.* **2024**, e202408592. <https://doi.org/10.1002/anie.202408592>.
- (14) Young, J. B.; Hughes, R. W.; Tamura, A. M.; Bailey, L. S.; Stewart, K. A.; Sumerlin, B. S. Bulk Depolymerization of Poly(Methyl Methacrylate) via Chain-End Initiation for Catalyst-Free Reversion to Monomer. *Chem* **2023**. <https://doi.org/10.1016/j.chempr.2023.07.004>.
- (15) Kubota, K.; Jiang, J.; Kamakura, Y.; Hisazumi, R.; Endo, T.; Miura, D.; Kubo, S.; Maeda, S.; Ito, H. Using Mechanochemistry to Activate Commodity Plastics as Initiators for Radical Chain

Reactions of Small Organic Molecules. *J. Am. Chem. Soc.* **2023**.  
<https://doi.org/10.1021/jacs.3c12049>.

- (16) Jung, E.; Cho, M.; Peterson, G. I.; Choi, T.-L. Depolymerization of Polymethacrylates with Ball-Mill Grinding. *Macromolecules* **2024**. <https://doi.org/10.1021/acs.macromol.3c02664>.
- (17) Stache, E. E.; Kottisch, V.; Fors, B. P. Photocontrolled Radical Polymerization from Hydridic C–H Bonds. *J. Am. Chem. Soc.* **2020**, *142* (10), 4581–4585. <https://doi.org/10.1021/jacs.0c00287>.
- (18) Whitfield, R.; Jones, G. R.; Truong, Nghia. P.; Manring, L. E.; Anastasaki, A. Solvent-Free Chemical Recycling of Polymethacrylates Made by ATRP and RAFT Polymerization: High-Yielding Depolymerization at Low Temperatures. *Angew. Chem.* **2023**, *135* (38), e202309116. <https://doi.org/10.1002/ange.202309116>.
- (19) Bartsch, M.; Schmidt-Naake, G. Application of Nitroxide-Terminated Polymers Prepared by Sonochemical Degradation in the Synthesis of Block Copolymers. *Macromol. Chem. Phys.* **2006**, *207* (2), 209–215. <https://doi.org/10.1002/macp.200500380>.
- (20) Degirmenci, M.; Catalgil-Giz, H.; Yagci, Y. Synthesis of Block Copolymers by Combined Ultrasonic Irradiation and Reverse Atom Transfer Radical Polymerization Processes. *J. Polym. Sci. Part Polym. Chem.* **2004**, *42* (3), 534–540. <https://doi.org/10.1002/pola.10879>.
- (21) Kerr, A.; Moriceau, G.; Przybyla, M. A.; Smith, T.; Perrier, S. Bis(Trithiocarbonate) Disulfides: From Chain Transfer Agent Precursors to Iniferter Control Agents in RAFT Polymerization. *Macromolecules* **2021**, *54* (14), 6649–6661. <https://doi.org/10.1021/acs.macromol.1c00565>.
- (22) Carta, M.; James, S. L.; Delogu, F. Phenomenological Inferences on the Kinetics of a Mechanically Activated Knoevenagel Condensation: Understanding the “Snowball” Kinetic Effect in Ball Milling. *Molecules* **2019**, *24* (19), 3600. <https://doi.org/10.3390/molecules24193600>.
- (23) Do, J.-L.; Frišćić, T. Mechanochemistry: A Force of Synthesis. *ACS Cent. Sci.* **2017**, *3* (1), 13–19. <https://doi.org/10.1021/acscentsci.6b00277>.

## Supplementary Information

### Instrumentation

*Nuclear Magnetic Resonance (NMR) Spectroscopy:*  $^1\text{H}$  NMR spectra were acquired at room temperature on a Bruker US 400 (400 MHz) NMR instrument. The chemical shifts of peaks in the NMR spectra were referenced to the residual solvent peak (7.26 ppm and 2.50 ppm for  $\text{CDCl}_3$  and *d*-DMSO respectively). Data was analyzed using MestreNova software.

*Size Exclusion Chromatography (SEC):* SEC chromatograms were acquired at room temperature on an Agilent 1260 Infinity II LC using a 50  $\mu\text{m}$  PL Gel column at ambient temperature, in line with a Wyatt Technologies DAWN8 light scattering detector, Optilab refractive index detector, and UV absorbance detector. All chromatograms were acquired in DMF and UV absorbance was recorded at 310 or 330 nm.

*UV-Visible Spectroscopy:* UV/Vis spectra were acquired at room temperature on a Cary 3500 Multicell UV-Vis Spectrophotometer. Scans were acquired from 200.00 -800.00 nm with an averaging time of 0.020 s.

*Thermogravimetric Analysis (TGA):* TGA experiments were performed on a TA TGA-55 analyzer coupled with an electrospray ionization mass spectrometer.

## Synthesis of Model Compound (1)

Bis(butyl trithiocarbonate)



A suspension of 60% sodium hydride (0.417 g, 10.4 mmol, 1.04 equiv.) in 24 mL of anhydrous diethyl ether was prepared in a flame-dried 100 mL round bottom flask. The flask was cooled to 0°C. Butanethiol (1.1 mL, 10.0 mmol, 1.0 equiv.) was added to the flask dropwise under N<sub>2</sub>. The reaction mixture was stirred for an additional 30 minutes at 0°C. Carbon disulfide (0.63 mL, 10.4 mmol, 1.04 equiv.) was subsequently added dropwise. The reaction was returned to room temperature and was left to stir for 3 hours. The mixture was precipitated in 25 mL of pentane. The resulting yellow solid was filtered and washed with additional pentane. The solid was dissolved in 15 mL of diethyl ether and cooled to 0°C under ambient conditions. Iodine (1.5 g, 5.5 mmol, 0.55 equiv.) was added over the course of 5 minutes. The reaction was allowed to stir overnight. The resultant red solid was removed via filtration. The filtrate was extracted with deionized water (1 x 20 mL), saturated aqueous sodium thiosulfate (3 x 20 mL), and brine (1 x 20 mL). The organic layer was collected, dried over sodium sulfate, and concentrated in vacuo to produce an orange oil. Additional purification through a basic alumina plug was performed as necessary. Yield: 75%.

<sup>1</sup>H NMR (400 MHz, CDCl<sub>3</sub>) δ = 3.30 (t, 4 H), 1.70 (p, 4 H), 1.45 (m, 4 H), 0.90 (t, 6 H)



**Figure S1.** Photograph of compound **1**, an orange oil.

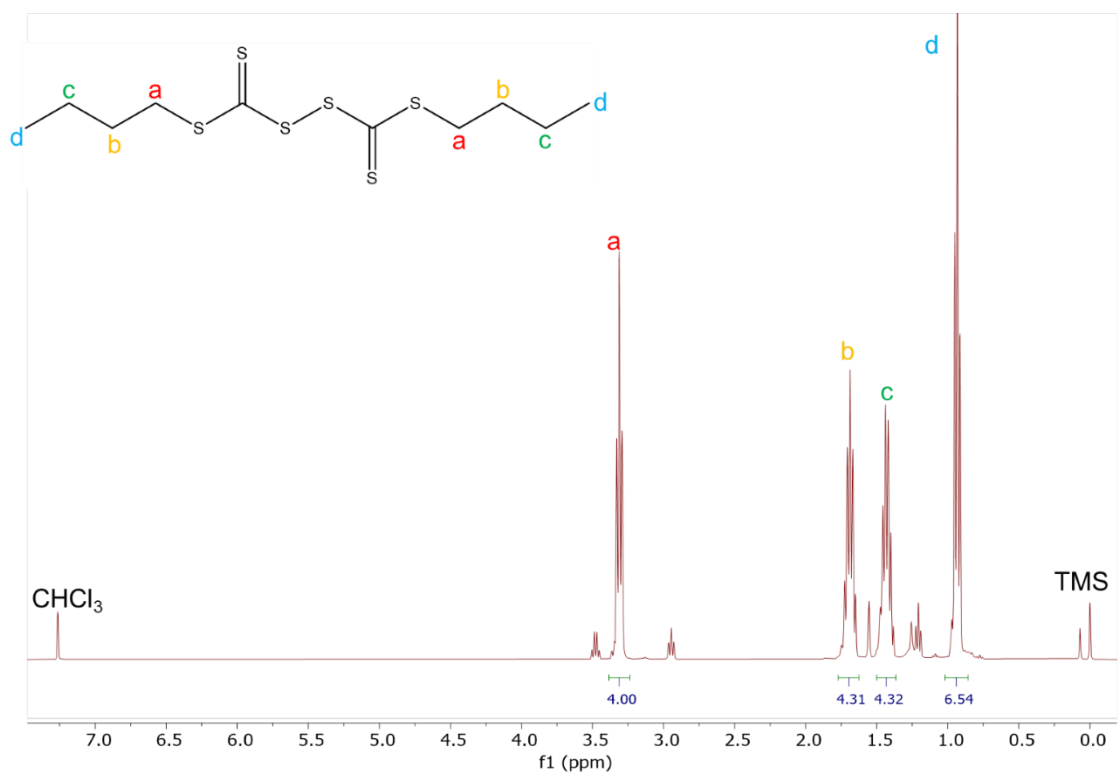


**Figure S2.** 1D <sup>1</sup>H NMR of compound **1**.

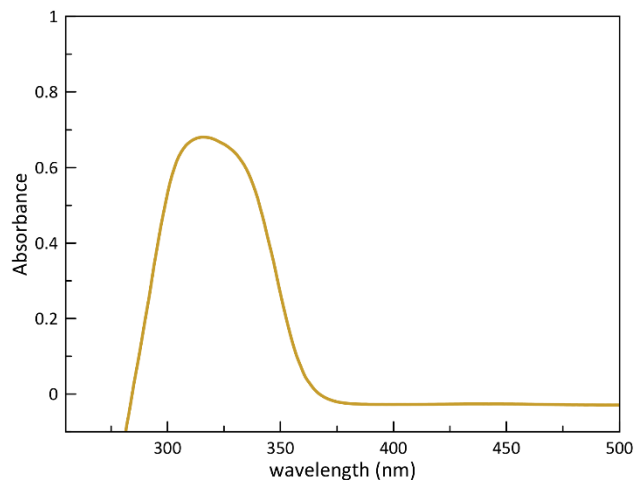
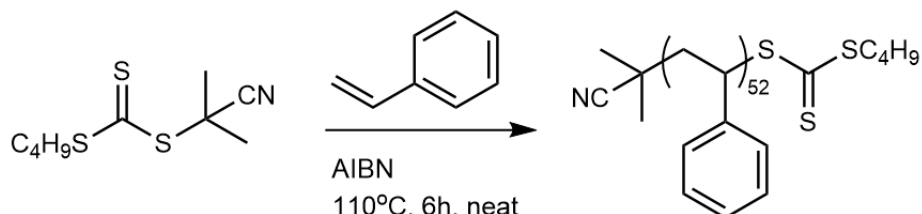


**Figure S3.** UV/Vis absorption spectrum of model compound **1**.

### Synthesis of Model Compound (3)

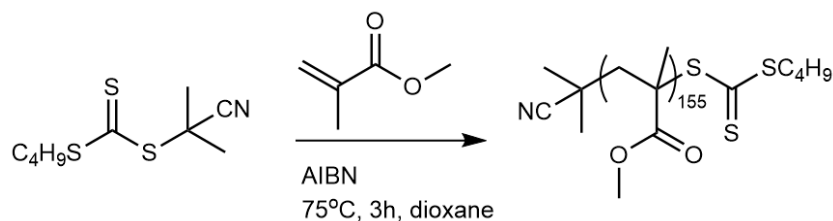
#### Polystyrene



In a Schlenk flask, styrene (10.42 g, 100 mmol, 100 equiv.), azobisisobutyronitrile (32 mg, 0.2 mmol, 0.2 equiv.), cyanopropyl butyl trithiocarbonate (233 mg, 1 mmol, 1 equiv.) were dissolved. The reaction mixture was degassed with nitrogen for 10 minutes. The flask was then heated at 110°C for 6 hours. To purify, the reaction mixture was precipitated three times into methanol and filtered. The product was a yellow powder. The precipitate was dried under vacuum at 45°C overnight.  $M_n = 5697 \pm 147$  Da.  $M_w = 5798 \pm 149$  Da.  $\mathcal{D} = 1.018 \pm 0.037$ .

## Synthesis of Model Compound (4)

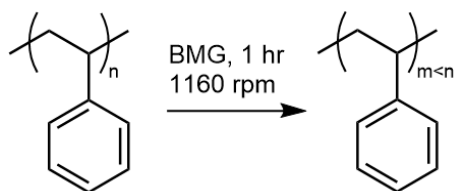
### Poly(methyl methacrylate)



In a Schlenk flask, methyl methacrylate (3.006 g, 30.03 mmol, 30 equiv.), azobisisobutyronitrile (16 mg, 0.096 mmol, 0.1 equiv.), cyanopropyl butyl trithiocarbonate (54.4 mg, 0.233 mmol, 1 equiv.) were dissolved in 1,4-dioxane (2 mL). The reaction mixture was degassed with nitrogen for 10 minutes. The flask was then heated at 75°C for 3 hours. To purify, the reaction mixture was precipitated three times into methanol and filtered. The product was a yellow powder. The precipitate was dried under vacuum at 45°C overnight.  $M_n = 15320 \pm 397$  Da.  $M_w = 15950 \pm 405$  Da.  $\bar{D} = 1.041 \pm 0.038$ .

## General Procedure for Ball Milling Experiments

### Polystyrene



280 kDa PS (100 mg – 1 g) was added to a stainless-steel ball milling jar with 35 g of 5 mm stainless-steel balls. The samples were ball milled for 10 minutes to 1 hour at 1160 rpm. The product was a white powder.

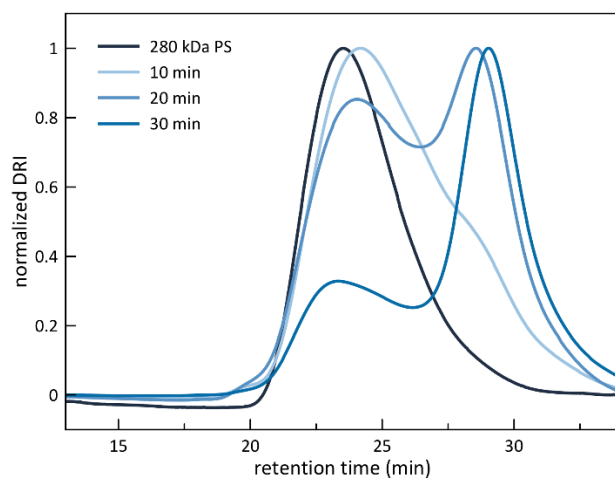


**Figure S4.** SEC chromatogram of 100 mg of PS after ball milling for 10 minutes, 20 minutes, and 30 minutes with 35 g of stainless-steel balls.

entry	mill time (min)	$M_n$ (kDa)	$M_w$ (kDa)	$\bar{D}$
1	0	150	280	1.9
2	10	44	177	4.02
3	20	43	147	3.40
4	30	25	86	3.43

**Table S1.** 100 mg of PS after ball milling for 10 minutes, 20 minutes, and 30 minutes with 35 g of stainless-steel balls.

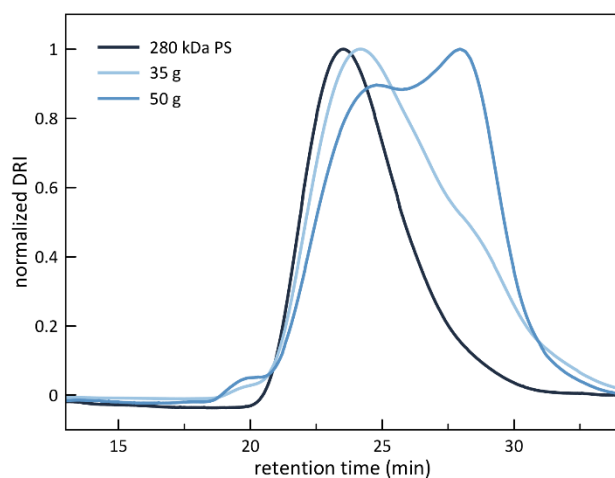


**Figure S5.** SEC chromatogram of 100 mg of PS after ball milling for 10 minutes with 35 g of stainless-steel balls and with 50 g of stainless-steel balls.

entry	ball mass (g)	$M_n$ (kDa)	$M_w$ (kDa)	$\bar{D}$
1	N/A	150	280	1.9
2	35	44	177	4.02
3	50	49	139	2.85

**Table S2.** 100 mg of PS after ball milling for 10 minutes with 35 g of stainless-steel balls and with 50 g of stainless-steel balls

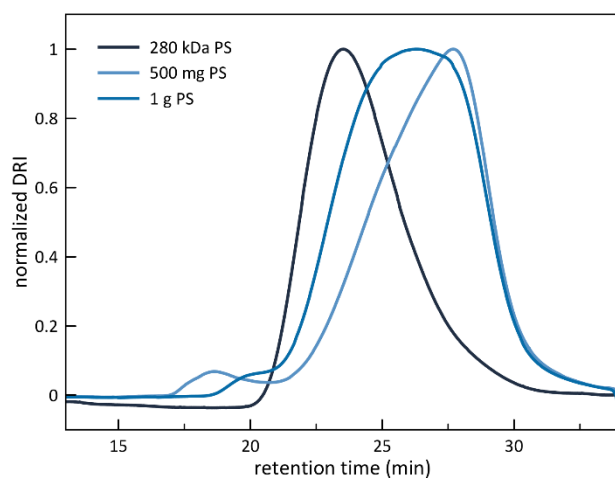
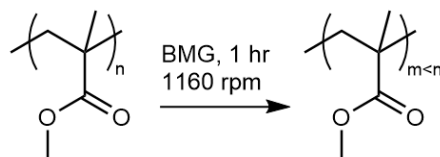


**Figure S6.** SEC chromatogram of PS after ball milling with 100 mg, 500 mg, and 1 g of PS for 60 minutes with 35 g of stainless-steel balls.

entry	polymer mass (g)	$M_n$ (kDa)	$M_w$ (kDa)	$\bar{D}$
1	N/A	150	280	1.9
2	0.5	43	85	1.97
3	1	52	117	2.26

**Table S3.** PS after ball milling with 100 mg, 500 mg, and 1 g of PS for 60 minutes with 35 g of stainless-steel balls.

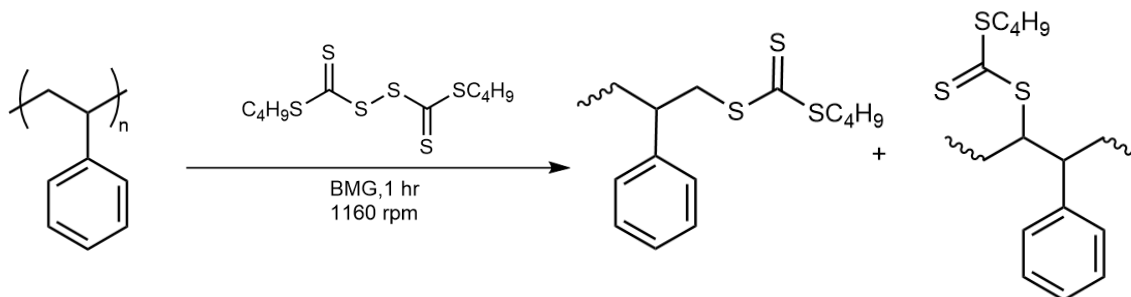
Poly(methyl methacrylate)



350 kDa PMMA (100 mg – 1 g) was added to a ceramic ball milling jar with 35 g of 5 mm ceramic balls. The samples were ball milled for 10 minutes to 1 hour at 1160 rpm. The product was a white powder.

## General Procedure for Ball Milling Radical Capture Experiments

### Polystyrene



280 kDa polystyrene (500 mg, 1 equiv.) and bis(butyl trithiocarbonate) (TTC) (50 mg, 10 wt%) were added to a stainless-steel ball milling jar with 35 g of 5 mm stainless-steel balls. The samples were ball milled for 1 hour at 1160 rpm. To purify, the reaction mixture was precipitated three times into methanol and filtered. The product was a white powder. The precipitate was dried under vacuum at 45°C overnight.

<sup>1</sup>H NMR (400 MHz, CDCl<sub>3</sub>) δ = 7.04 (m, 3n H), 6.57 (m, 2n H), 3.24 (q, 2H), 1.83 (m, 1n H), 1.54 (m, 2n H), 0.88 (t, 3H)

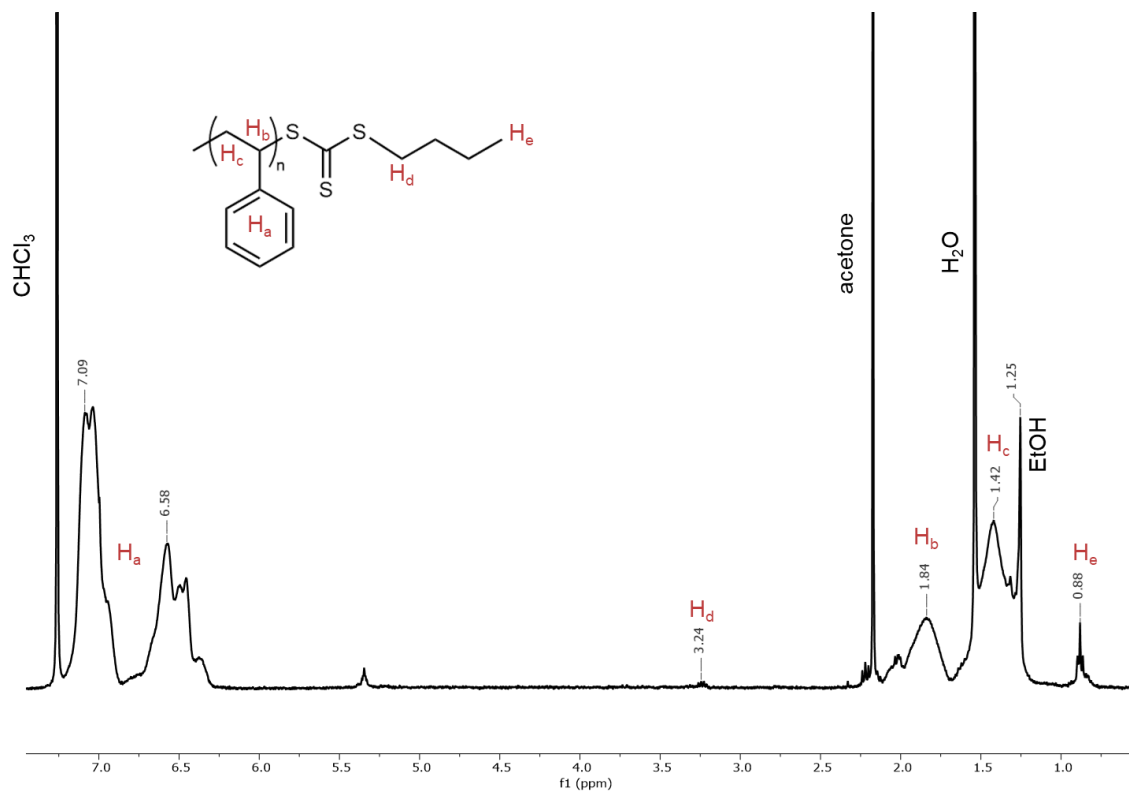


**Figure S7.** 1D  $^1\text{H}$  NMR of compound 5.

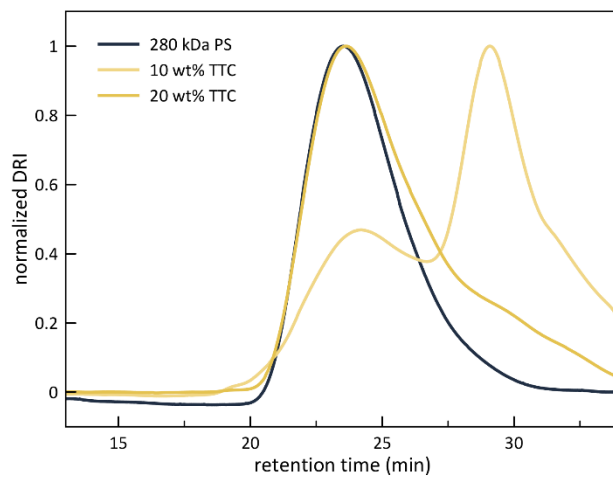


**Figure S8.** SEC chromatogram of 100 mg of PS after ball milling with 10 wt%, 20 wt%, and 50 wt% TTC with 35 g of stainless-steel balls for 1 hour.

entry	wt% TTC	% incorporation	$M_n$ (kDa)	$M_w$ (kDa)	$\bar{D}$
1	N/A	0	150	280	1.9
2	10	45%	16	104	6.20
3	20	109%	66	227	3.43

**Table S4.** 100 mg of PS after ball milling with 10 wt%, 20 wt%, and 50 wt% TTC with 35 g of stainless-steel balls for 1 hour.

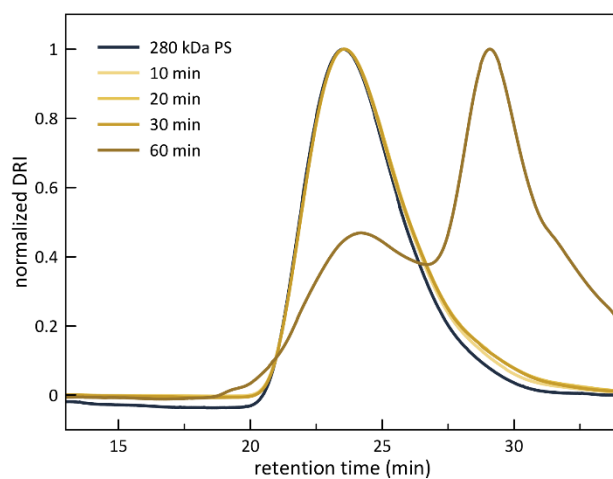


**Figure S9.** SEC chromatogram of 100 mg PS after ball milling with 10 wt% TTC for 10 minutes, 20 minutes, 30 minutes, and 1 hour with 35 g of stainless-steel balls.

entry	mill time (min)	% incorporation	M <sub>n</sub> (kDa)	M <sub>w</sub> (kDa)	Đ
1	N/A	0	150	280	1.9
2	10		126	267	2.12
3	20		131	273	2.08
4	30		141	275	1.95
5	60	45%	16	104	6.20

**Table S5.** 100 mg PS after ball milling with 10 wt% TTC for 10 minutes, 20 minutes, 30 minutes, and 1 hour with 35 g of stainless-steel balls.

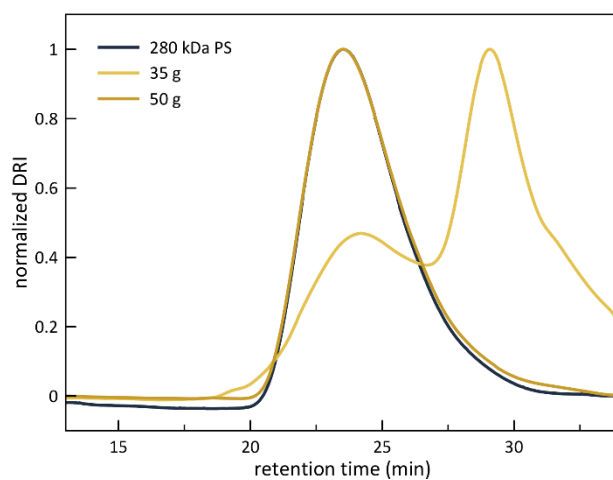


**Figure S10.** SEC chromatogram of 100 mg of PS after ball milling with 10 wt% TTC with 35 g and 50 g of stainless-steel balls for 1 hour.

entry	ball mass (g)	% incorporation	M <sub>n</sub> (kDa)	M <sub>w</sub> (kDa)	Đ
1	N/A	0	150	280	1.9
2	35	45%	16	104	6.20
3	50		123	267	2.16

**Table S6.** 100 mg of PS after ball milling with 10 wt% TTC with 35 g and 50 g of stainless-steel balls for 1 hour.

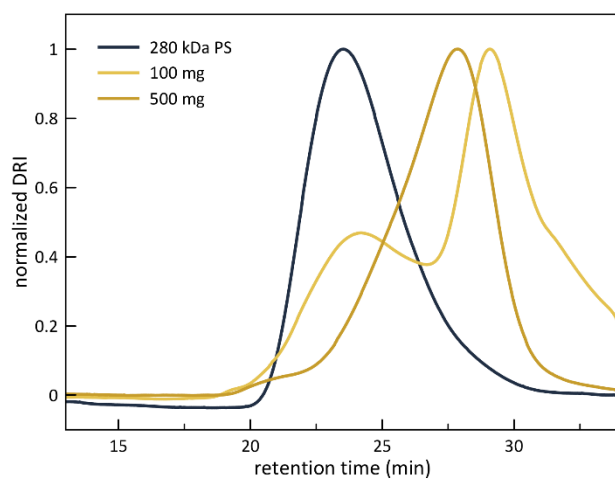
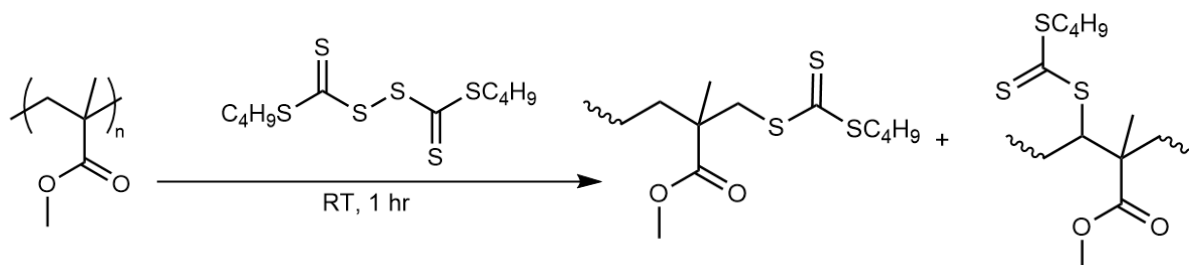


**Figure S11.** SEC chromatogram of PS after ball milling with 100 mg and 500 mg of PS with 10 wt% TTC and 35 g of stainless-steel balls.

entry	polymer mass (mg)	% incorporation	M <sub>n</sub> (kDa)	M <sub>w</sub> (kDa)	Đ
1	N/A	0	150	280	1.9
2	100	45%	16	104	6.20
3	500	108%	41	76	1.83

**Table S7.** PS after ball milling with 100 mg, 200 mg, 500 mg, and 1 g of PS with 10 wt% TTC and 35 g of stainless-steel balls.

Poly(methyl methacrylate)



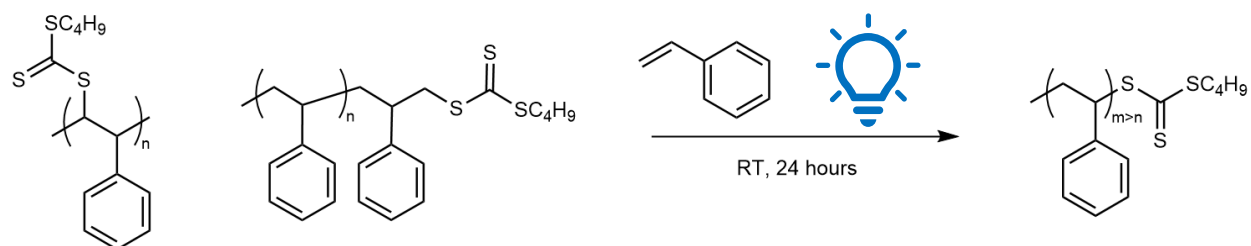
350 kDa poly(methyl methacrylate) (500 mg, 1 equiv.) and bis(butyl trithiocarbonate) (TTC) (50 mg, 10 wt%) were added to a ceramic ball milling jar with 35 g of 5 mm ceramic balls. If milled with monomer, methyl methacrylate (40  $\mu$ L, 240 equiv.) is also added to the jar. The samples were ball milled for 2 hours at 1160 rpm. To purify, the reaction mixture was precipitated three times into methanol and filtered. The product was a white powder. The precipitate was dried under vacuum at 45°C overnight.

#### General Procedure for Ultrasonication Radical Capture Experiments

A circulating pump was assembled to ensure constant temperature of the ultrasonicated solution. A 5 mg mL<sup>-1</sup> solution of polymer was prepared in toluene with 350 equivalents of TTC. The solution was sonicated at 100% amplitude (120  $\mu$ m) and 20 kHz for 1 hour, with the on/off pulse set to 40 seconds on and 20 seconds off. To purify, the reaction mixture was precipitated three times into methanol and filtered. The product was a white powder. The precipitate was dried under vacuum at 45°C overnight.

#### General Procedure for Photoinitiated Chain Extension of Polystyrene

Polystyrene



Styrene (0.521 g, 5.0 mmol) and ball milled PS (38.2 mg) were dissolved in a Schlenk flask. The reaction mixture was degassed with nitrogen for 10 minutes. The flask was irradiated in a blue light photoreactor for 24 hours at room temperature. To purify, the reaction mixture was precipitated three times into methanol and filtered. The product was a white powder. The precipitate was dried under vacuum at 45°C overnight.

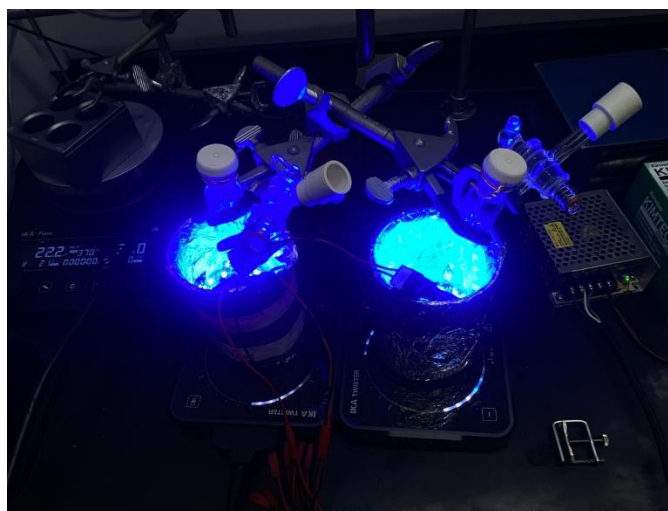


**Figure S12.** Reaction set up for green light polymerization.

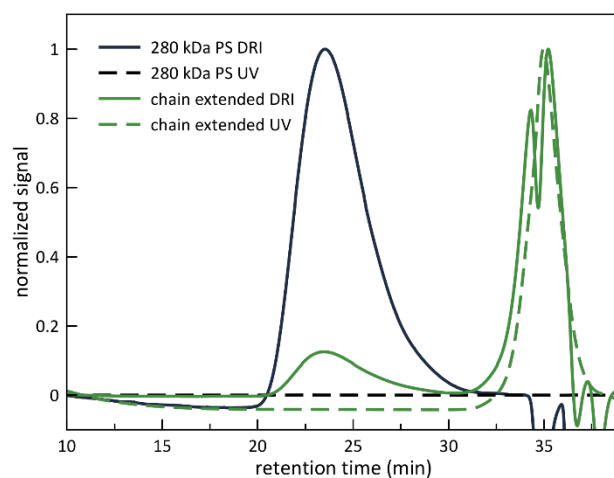


**Figure S13.** SEC chromatograms of chain extension of 280 kDa PS (control experiment).

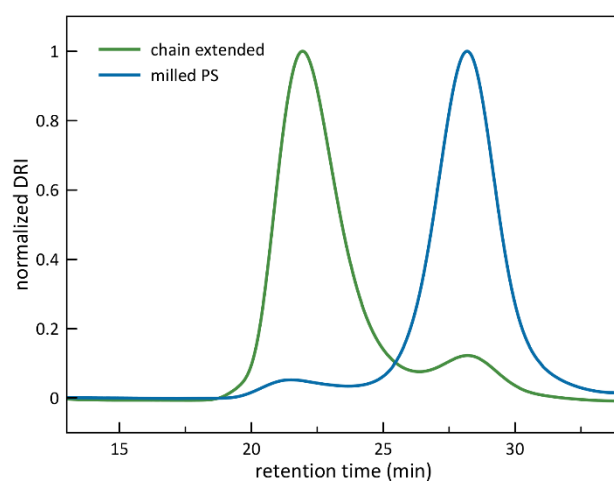


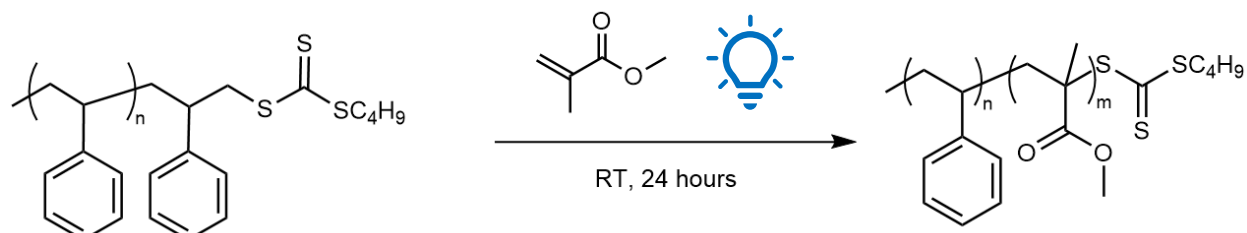
**Figure S14.** SEC chromatograms of chain extension of milled PS (control experiment).

entry	polymer	$M_n$ (kDa)	$M_w$ (kDa)	$\bar{D}$
1	280 kDa PS	150	280	1.9
2	Milled with TTC	41	76	1.83
3	Chain Extended	160	307	1.93

**Table S8.** Chain extension of PS milled with TTC.

## General Procedure for Photoinitiated Chain Extension of Polystyrene with Methyl methacrylate

Poly(styrene-*co*-methyl methacrylate)



In a Schlenk flask, methyl methacrylate (0.501 g, 5.0 mmol) and ball milled PS (66.8 mg) were dissolved in 0.74 mL of 1,4-dioxane. The reaction mixture was degassed with nitrogen for 10 minutes. The flask was irradiated in a blue light photoreactor for 24 hours at room temperature. To purify, the reaction mixture was precipitated three times into methanol and filtered. The product was a white powder. The precipitate was dried under vacuum at 45°C overnight.

### **GPC-UV Calibration Curve for Quantification of TTC Functionalization**

Five calibration solutions of a model 5.7 kDa PS with one TTC end group per chain were made in DMF: 10 mg mL<sup>-1</sup>, 5.0 mg mL<sup>-1</sup>, 1.0 mg mL<sup>-1</sup>, 0.50 mg mL<sup>-1</sup>, and 0.10 mg mL<sup>-1</sup>. GPC coupled with UV detection at 310 nm and 330 nm was performed on each calibration solution. The resultant peak area of the UV trace was plotted as a function of TTC concentration ( $R^2 > 0.999$ ). This calibration curve was used to determine TTC concentration of unknown ball milled samples based on the peak area of the UV signal at either 310 nm or 330 nm.

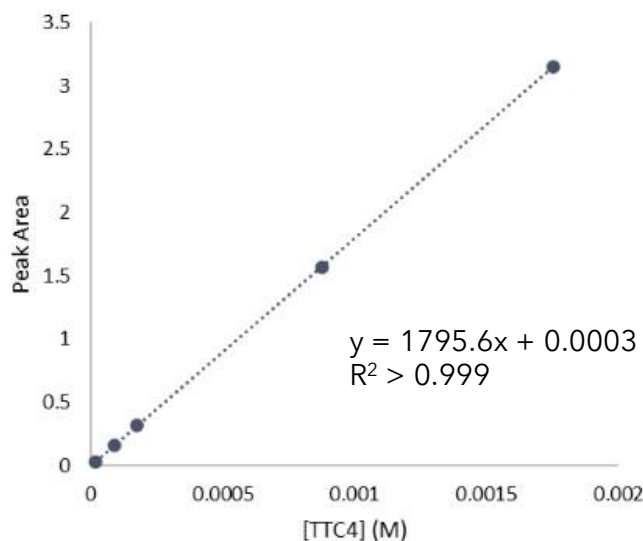


**Figure S15.** Calibration curve plotting peak area of absorbance at 310 nm of the model polymer as a function of TTC concentration.

### Protein Conjugate Analysis on GPC-UV for Quantification of TTC Functionalization

To perform this analysis, the  $dn\ dc^{-1}$  and the  $\epsilon$  of both the polymer and the modifier (TTC) must be known. The  $dn\ dc^{-1}$  of PS in DMF is reported in the literature to be 0.14. The extinction coefficient at 310 nm was determined by GPC-UV to be 0.005. The  $dn\ dc^{-1}$  of bis(butyl trithiocarbonate) was determined by the batch injection method on the GPC-UV. Five calibrator solutions were injected into the RI detector through syringe infusion, and the batch  $dndc$  method was applied. The  $dn\ dc^{-1}$  of bis(butyl trithiocarbonate) was determined to be  $0.1897\ mL\ g^{-1}$ . The extinction coefficient at 310 nm was determined by UV/Visible spectroscopy to be  $66.8\ mL\ mg^{-1}\ cm^{-1}$ . The protein conjugate method was then applied to a functionalized polymer. These values were input, and the protein fraction (mass fraction of polymer) was then determined.